[논문] 열처리공학회지, 제24권 제1호(2011)
J. of the Korean Society for Heat Treatment, *Vol. 24, No. 1, (2011) pp. 16~22*

A Study on the Microstructures and Electromagnetic Properties of Al-Co/AlN-Co Thin Films

Chang-Suk Han†, Seung-Oh Han*

Dept. of Defense Science & Technology, Hoseo University
**Institute of Fusion Technology, Hoseo University, 165 Sechul-Ri, Baebang-Myun, Asan City, Chungnam 336-795, Korea*

Abstract Al-Co/AlN-Co multilayer films with different layer thicknesses were prepared by using a two-facing target type D.C sputtering (TFTS) system. The deposited films were annealed isothermally at different temperatures and their microstructure, magnetic properties and resistivity were investigated. The magnetization of as-deposited films is very small irrespective of layer thickness. It was found that annealing conditions and layer thickness ratio (LTR) of Al-Co to AlN-Co can control the microstructure as well as the physical properties of the prepared films. The resistivity and magnetization increase and the coercivity decreases with decreasing LTR. High resistivity and sufficient magnetization were obtained for the films with LTR = 0.35. Films having such considerable magnetization and resistivity will be a potential candidate to be used for a high density recording material.

(Received October 29, 2010; Accepted November 22, 2010)

Key words : *microstructure, magnetization, resistivity, coercivity, layer thickness*

1. Introduction

Recent high technology developments of electronic devices have led to a demand for miniaturization of magnetic devices, operating at frequencies higher than 50 MHz [1, 2]. Such devices require that magnetic materials have a sufficiently large electric resistivity ρ and are in the form of thin films, in order to suppress eddy current losses. In order to solve those problems, high resistive metal films possessing a very fine two-phase hetero-amorphous structure have been studied, and magnetic granular system, where magnetic particles are embedded in an insulator matrix, has also been studied [3-5]. The authors reported the microstructure and magnetic and electrical properties of AlN-Co thin films in the previous study [6]. These films showed high resistivity and sufficient saturation magnetization, and the coercivity of the films was 22~94 Oe at a magnetic field of 1 kOe. Moreover, it was found that multilayer films show better soft magnetic properties than monolayer films [7, 8]. An ideal high-density recording magnetic material must have high permeability, high electric resistivity, large saturation magnetization coupled with low energy loss and also a high corrosion resistance. This is why we used AlN as a high resistive and high corrosion resistance insulator matrix and Co as a magnetic particle embedded or dispersed in that matrix. And Al-Co inter layer in the multilayer was used to control grain growth which will result in smaller coercivity. In this paper, a new approach for preparing Al-Co/AlN-Co multilayer films by a TFTS is described. We investigate the formation of Al-Co/AlN-Co films and compare their microstructure, magnetic property and electrical resistivity with those of the AlN-Co films.

2. Experimental Procedure

Predetermined conditions were applied to prepare Al-Co/AlN-Co thin films [6]. In this work, an Al (99.95% pure) target of 100 mm diameter and 5 mm thickness was used as an upper target while a

†E-mail : hancs@hoseo.edu

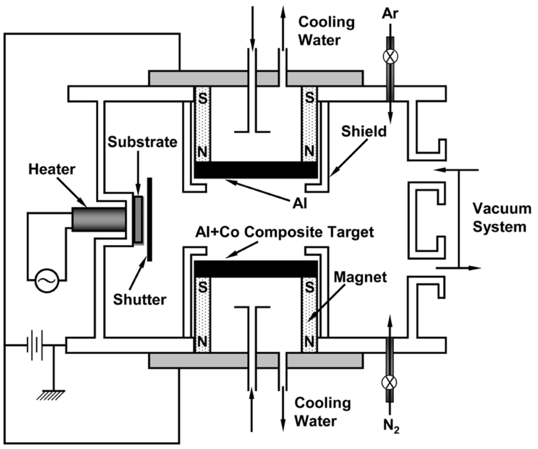

Fig. 1. Schematic drawing of a Two-Facing-Target-Type sputtering (TFTS) apparatus.

composite target of Al (99.95%) and Co (99.98%) with an area fraction of Co(Co/(Al + Co)) = 0.087 (referred as to TAF) was used as a lower target (Fig. 1). Corning glass (7059) was mostly used as a substrate. Substrate temperature was lower than 310 K. Target voltage was between -300 V and -500 V (DC). Sputtering currents were 400 mA and 200 mA for the deposition of AlN-Co and Al-Co layers, respectively. N_2 partial gas pressures of 0.052 and 0 were used for the deposition of AlN-Co and Al-Co layers, but the total gas pressure was fixed at 0.4 Pa for both layers. The initial pressure of the chamber was lower than 2×10^{-4} Pa. The total thickness of the films varied from 880 nm to 550 nm. Films having a wide range of layer thickness (10~30 nm for AlN-Co layer and 3.5~80 nm for Al-Co inter layer) were prepared and studied. As-deposited films were annealed isothermally in a vacuum of 2.6×10^{-4} Pa at different temperatures. The microstructure of thus prepared films was examined by X-ray diffraction (XRD), and electron microscopy observations (TEM, HRTEM, X-TEM, NBD). Atomic percentage of the contents of the films was checked by electron dispersive spectroscopy (EDS), as listed in Table 1. Magnetic and electrical properties were measured by a vibrational sample magnetometer (VSM) and the four probe method respectively. All the measurements were performed at room temperature (RT).

3. Results and Discussion

3.1. As-deposited films

3.1.1 Microstructure

The microstructure of Al-Co/AlN-Co films strongly depends on the ratio of layer thickness of Al-Co layer. Fig. 2 shows X-ray profiles for films deposited with a Co target area fraction of 0.087 with different LTR's. The profile for LTR = 2.7 ((Al-Co) 80 nm/(AlN-Co) 30 nm) shows two broad peaks: first one around the angular position of $2\theta\sim36^{\circ}$, which is for 0002 peak of AlN and the other one around the angular position of $2\theta\sim44^{\circ}$, which is for the peaks of β-Co 111 and also peaks ascribed to the compounds of AlCo. With decreasing LTR (0.7 in Fig. 2(b) and 0.35 in Fig. 2(c)), the second peak becomes broader, while the first peak is still intact. Fig. 3 shows cross-sectional TEM images for as-deposited films with a LTR = 2.7 ((Al-Co) 80 nm/(AlN-Co) 30 nm). Alterna-

Table 1. Properties of as-deposited films

Kind of film	TAF of Co (Co at% (approx.))	Magnetization emu/cm^3	Resistivity μ-Ω-cm
AlN-Co	0.047(20 at%)	3.5 ~ 5.0	2500 ~ 2900
AlN-Co	0.087(25 at%)	1.5 ~ 6.0	990 ~ 1360
$(Al\text{-}Co)_{80nm}/(AlN\text{-}Co)_{30nm}$	0.087	1.7 ~ 2.9	~ 600
$(Al\text{-}Co)_{12nm}/(AlN\text{-}Co)_{15nm}$	0.087	5.7 ~ 8.5	~ 800
$(Al\text{-}Co)_{7nm}/(AlN\text{-}Co)_{10nm}$	0.087	0.8 ~ 2.6	~ 830
$(Al\text{-}Co)_{3.5nm}/(AlN\text{-}Co)_{10nm}$	0.087	3.5 ~ 5.0	~ 970

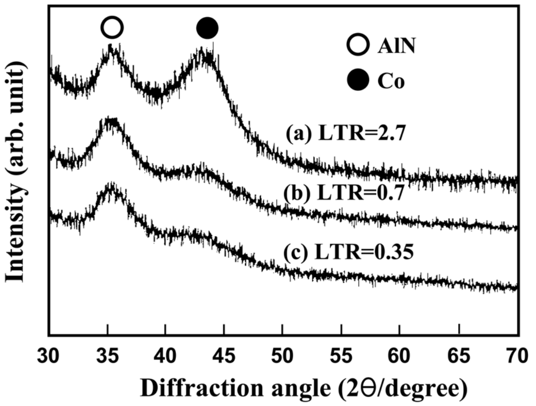

Fig. 2. Typical XRD profiles of as-deposited films with different LTR's.

tive stacking of AlN-Co/Al-Co layers appears clearly. The existence of the growth of a vivid interfacial ultrathin layer is also seen. Fig. 3(b) shows the aging effect on such a thin film which was aged for 15 days after thinning. Drastic changes of microstructure including changes in layer thickness were observed clearly. Both the layers expand and particles of AlCo compound grow during aging in the Al-Co layer. The layer expansion is probably due to the release of film stress enhanced by aging at RT because of the film being ultra-thin.

3.1.2 Magnetic property and electrical resistivity

For all the as-deposited films, the magnetization is too small irrespective of LTR of the films. This may be due to the fact that in as-deposited films Co is not in crystalline state, and/or its Curie temperature decreases below room temperature. This is not clear yet. The resistivity increases with decreasing LTR on account of decreasing in volume fraction of the conducting elements in the films. Numerical results for magnetization and resistivity for different films are summarized and listed in Table 1.

3.2. Effect of Heat Treatment

3.2.1 Microstructure

Microstructural change and phase separation depend on annealing conditions. When a film with LTR = 2.7 was annealed at 673 K for 120 ks, three phases of AlN, AlCo and β-Co are detected (Fig. 4(b)), but when annealed at 773 K for the same period, they crystallize into five distinct phases of AlN, AlCo, Co_2Al_5, α-Co and β-Co (Fig. 4(a)). Among these phases, a related AlCo phase is temporarily identified to be an ordered AlCo phase, although it was not confirmed clearly. Three phases of AlN, AlCo and β-Co were detected for a film with LTR = 0.7 ((Al-Co)7 nm/(AlN-Co) 10 nm), annealed at 773 K for 120 ks (Fig. 4(c)), where the peaks for individual phases are broad for lower annealing temperatures (Fig. 4(d)). On the other hand, for a film with lower LTR = 0.35 ((Al-Co) 3.5 nm/(AlN-Co) 10 nm), only two phases of AlN and β-Co are detected and no phase ascribed to the compounds of

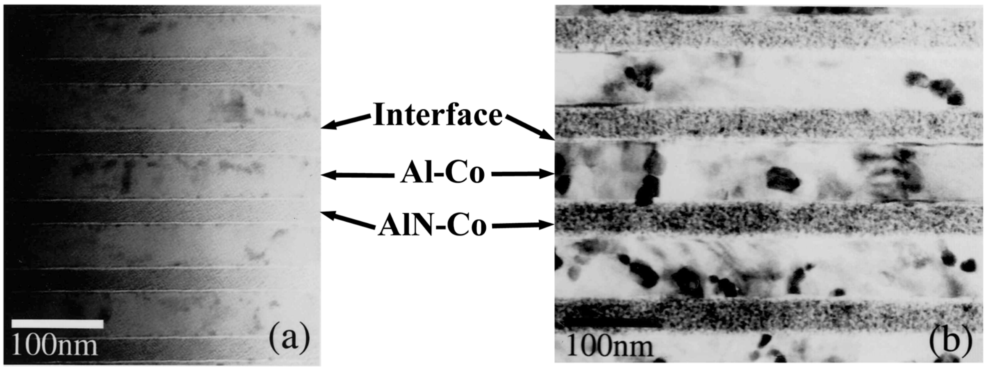

Fig. 3. Cross-sectional TEM images of as-deposited film with LTR = 2.7; (a) just after ion thinning, (b) aged for 15 days.

AlCo is seen under the same annealing conditions (Fig. 4(e)) and the peaks are broader at 623 K (Fig. 4(f)).

Fig. 5 shows TEM micrographs and electron diffraction pattern for an annealed film with LTR = 2.7. Fig. 5(a) reveals that the layer and the interfacial growths are still intact just after annealing, But we can observe large precipitates in Al-Co layers and fine particles in AlN-Co layers. Fig. 5(b) shows the microstructure of the same ion-thinned film observed after aging for 15 days. Such particles coarsened to grow larger in both the layers. Another finding is that the layer thickness increases, probably due to the further release of film stress during aging. Fig. 5(c) is a high resolution image taken from the indicated particle of the aged film and Fig. 5(d) is the corresponding nano beam diffraction (NBD) from such a particle.

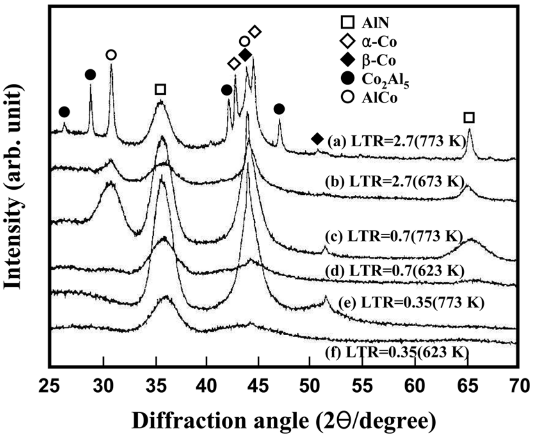

Fig. 4. Typical XRD profiles of films with different LTR's, annealed at different temperatures for 120 ks.

3.2.2 Magnetic property

Magnetic properties of annealed films change in accordance with the changes in microstructure. Fig. 6 shows the saturation magnetization as a function of annealing time at different annealing temperatures for the films with different LTR's. The magnetization is mainly dependent on annealing temperatures: it is larger at higher annealing temperatures for the films with the same LTR. However, it increases with decreasing LTR. A drastic change in magnetization occurs before 10.8 ks of annealing, and then the increment is moderate. For the films with LTR = 2.7, the magnetization is almost steady after 10.8 ks when annealed at 673 K.

But when the film is annealed at 773 K, its magnetization slightly decreases with annealing

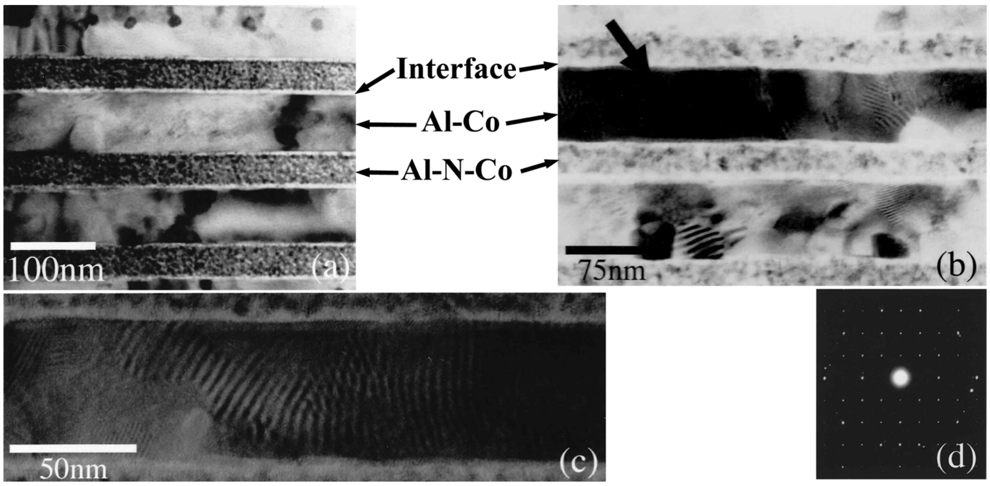

Fig. 5. Cross-sectional TEM images of a film with LTR = 2.7 annealed at 773 K for 120 ks; (a) just after ion thinning, (b) aged for 15 days, (c) high resolution image taken from the indicated portion and (d) nano-beam diffraction patterns taken from such an indicated portion.

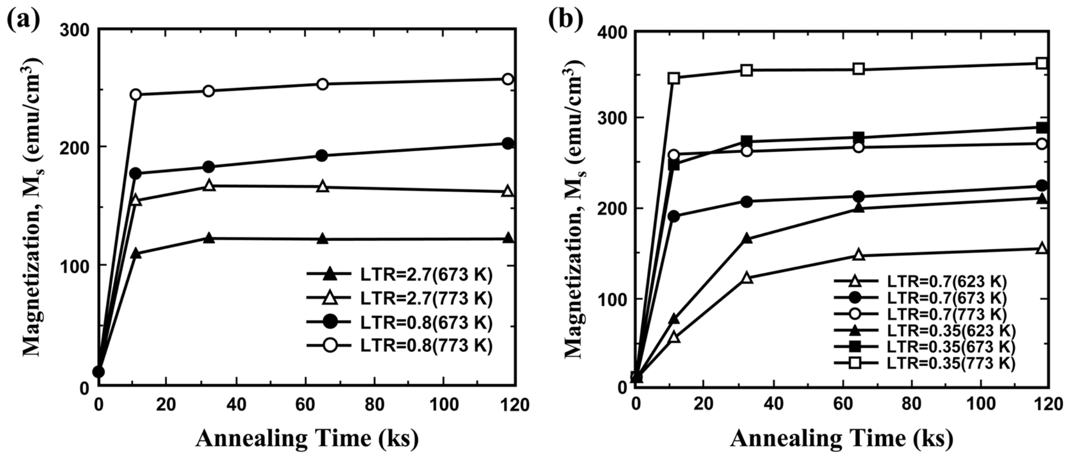

Fig. 6. Magnetization as a function of annealing time at different annealing temperatures for different LTR's films.

Table 2. Properties of annealed films

Kind of film	TAF of Co (Co at%(approx.))	Magnetization (emu/cm^3)	Coercivity (Oe)	Resistivity (μ-Ω-cm)
AlN-Co	0.047 (20 at%)	~ 260	90 ~ 95	~ 11×10^5
AlN-Co	0.087 (25 at%)	~ 360	20 ~ 90	~ 2200
$(Al\text{-}Co)_{80nm}/(AlN\text{-}Co)_{30nm}$	0.087	~ 162	22 ~ 73	~ 170
$(Al\text{-}Co)_{12nm}/(AlN\text{-}Co)_{15nm}$	0.087	~ 260	15 ~ 50	~ 770
$(Al\text{-}Co)_{7nm}/(AlN\text{-}Co)_{10nm}$	0.087	~ 270	15 ~ 59	~ 850
$(Al\text{-}Co)_{3.5nm}/(AlN\text{-}Co)_{10nm}$	0.087	~ 360	5 ~ 46	~ 2520

time after the same period (Fig. 6(a)). This can be explained by the microstructural changes of the films as follows: the phase separation is dominant at higher temperatures than at lower temperatures, and it progresses with annealing time (Fig. 4(a), (b)). The progress of the formation of AlCo and Co_2Al_5 compounds, whose magnetic moments are considered to be lower than those of the pure Co phases, decreases the magnetization with increasing annealing time. The highest magnetization of about 360 emu/cm^3 was obtained for a film with LTR = 0.35 (Fig. 6(b)), annealed at 773 K for 120 ks. This phenomenon can be also explained in terms of the changes in microstructure caused by annealing. This film have the thinnest Al-Co inter layer among the films examined and its corresponding XRD profile (Fig. 4(e)) shows that the film separates into the phases of AlN and Co, but no trace for AlCo and Co_2Al_5 compound formation is detected. As annealing time and temperature increase the separation of Co phases from AlN-Co layer becomes more dominant, and the crystallinity of Co phases becomes more and more improved [6]. Thus, the Co phases dispersed in the AlN matrix of the AlN-Co layers leads to an increase of the magnetization in such films. The coercivity decreases with decreasing layer thickness and LTR. It was observed that the coercivity decreases for low annealing temperatures for the same LTR films. The numerical values of coercivity are summarized and listed in Table 2.

3.2.3 Electrical resistivity

The resistivity of Al-Co/AlN-Co multilayer films having different LTR's was examined for different

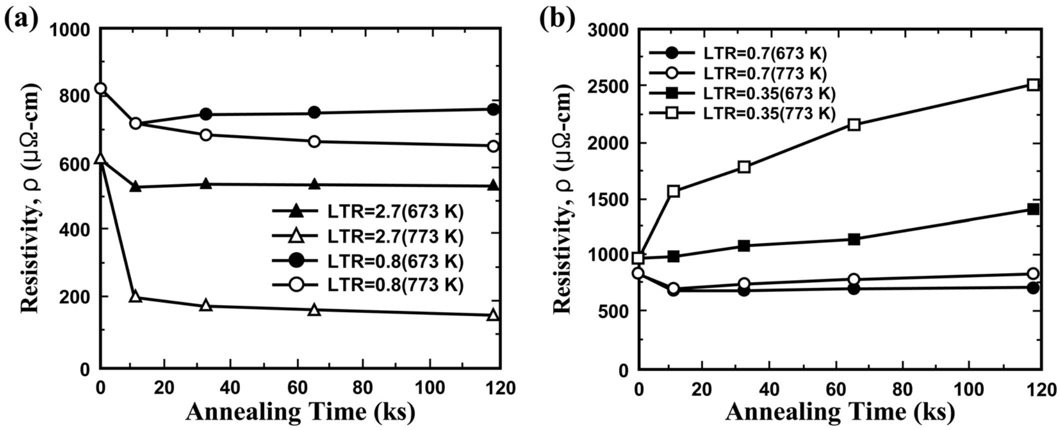

Fig. 7. Resistivity as a function of annealing time at different annealing temperatures for different LTR's films.

isothermal annealings. It was found that the resistivity is strongly dependent on LTR and also on the change of microstructure. Fig. 7 shows the resistivity as a function of annealing time at different temperatures for different LTR films. It is clear from the figure that a dominant change in resistivity occurs before 10.8 ks annealing and then the change is moderate for all the films. For the films higher than LTR = 2.7, the resistivity decreases with increasing annealing time and temperature, and the decrement is sharp at higher temperatures (Fig. 7(a)). This is probably due to the fact that at higher temperatures the phase separation is dominant and rapid formation of AlCo and Co_2Al_5 compounds (Fig. 4(a)), which make connecting networks with Co particles, decreases the resistivity. For the films with LTR = 0.8, the resistivity decreases throughout the annealing period at 773 K, but when annealed at 673 K the resistivity first decreases up to 10.8 ks and then slowly increases with annealing time (Fig. 7(a)).

As shown in the Fig. 7(b), for the films with LTR = 0.7 the resistivity first decreases and then increases with annealing time and temperature. On the contrary, for the films with LTR = 0.35, the resistivity increases throughout the annealing period with increasing annealing time and temperatures, and the increment is large at higher temperatures. This is mainly due to structural changes in AlN-Co layers caused by annealing: nano-crystallites of Co phase may be dispersed homogeneously in AlN-Co layers, resulting in low coercivity and in high magnetization with large resistivities, as shown in Table II. The highest resistivity of 2500 μΩ-cm was obtained for a film with LTR = 0.35, annealed at 773 K for 120 ks. In this connection, the XRD profile (Fig. 4(e)) of the film with LTR = 0.35 (the thinnest Al-Co inter layer) reveals that the film separates into the phases of AlN and Co, no appreciable trace for AlCo and Co_2Al_5 compound formation is detected. As explained in the previous section, the dispersed Co phases in the AlN insulator matrix of the AlN-Co layers leads to the increase of the resistivity in the film. The properties of annealed films examined are summarized and tabulated in Table 2.

4. Conclusions

A new approach was introduced for preparing Al-Co/AlN-Co multilayer films prepared by a TFTS system. The deposited films were annealed isothermally at different temperatures and their microstructure, magnetic properties and resistivity were investigated. The main results are summarized as follows:

1. This TFTS method is suitable for preparing Al-Co/AlN-Co multilayer films with different LTR's.

2. Annealing conditions, layer thickness and LTR can adjust the microstructure as well as the physical properties of the prepared films.

3. The resistivity and magnetization increase and the coercivity decreases with decreasing LTR.

4. High resistivity of 2500 μΩ-cm, a magnetization of 360 emu/cm^3 and a coercivity of 5 Oe were obtained for the films with LTR = 0.35.

References

1. L. N. Kotov, V. K. Turkov and V. S. Vlasov : J. Mag. & Mag. Mater., **316** (2007) 20.
2. R. Schwarz, M. Fernandes and J. Martins : Sensors and actuators. A, Physical, **115** (2004) 331.
3. H. Karamon : J. Appl. Phys., **63** (1988) 4306.
4. H. Fujimori : IEEE Trans. Magn., **30** (1994) 4779.
5. L. Maya, W. R. Allen, A. L. Glover and J. C. Mabon : J. Vac. Sci. Tech., **13B** (1995) 361.
6. C. S. Han and S. O. Han : submitted to J. Kor. Heat Treatment.
7. S. Yaegashi, T. Kurihara and K. Satoh : J. Appl. Phys., **81** (1997) 6303.
8. Z. Yuan, J. Shi and B. Xu : Plasma Sci. & Tech., **10** (2008) 446.